

# NONLINEAR IMAGE PROCESSING FOR AUTOMATIC INSPECTION OF RAILROAD LINES

*I. Khandogin, A. Kummert*

Laboratory for Communication Theory  
Department of Electrical Engineering  
University of Wuppertal  
Fuhrlrottstr. 10  
D - 42097 Wuppertal  
Germany  
Phone: +49-202-439-2961  
Fax: +49-202-439-2959

*D. Maiwald*

STN ATLAS Elektronik GmbH  
Simulation Division  
D - 28305 Bremen  
Germany  
Phone: +49-421-4573001  
Fax: +49-421-4573903

## ABSTRACT

Nonlinear image processing algorithms are important tools for solving sophisticated problems in the domain of image analysis. In particular, they are a useful and powerful alternative to linear filtering if objects have to be detected in real time on the basis of geometrical properties. In the following part, a nonlinear image processing system designed for the automatic inspection of rail surfaces by means of on-line analysis of video sequences is presented. The inspection of the fixing devices and other components of the track are not considered here. In our application, nonlinear operations are used for image enhancement, normalization, detection of damaged areas on the rail head and filtering of time series. This paper addresses practical aspects and advantages of equalizing image histograms, morphological filtering, binarization of images, and median filtering.

## 1. INTRODUCTION

In future, railroad lines will have to be checked automatically for defects on the rail surface. An attractive solution for the task is given by a video sensor unit and an on-line analysis system that are mounted on an inspection vehicle (cf. Fig. 1). The first consists of a light source and a high speed line camera and is designed for speeds of up to 100 km/h of the inspection vehicle [9]. The subsequent analysis system incorporates image processing chips and boards and a host computer. It is able to localize the rail head in the video images and to detect surface defects on it in real time. Finally, the analysis results are displayed on a monitor (cf. Figs. 1 and 2).

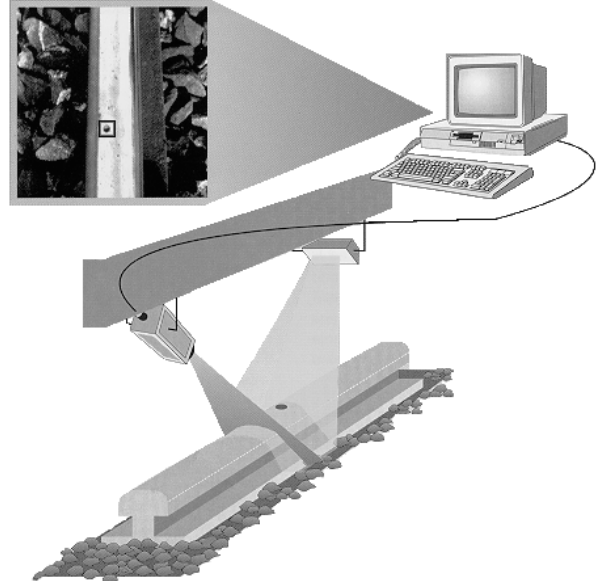


Fig. 1: Video sensor [9]

Fig. 2 shows an example of one video image where the analysis results are displayed by white vertical lines for foot and rail head and by a black circle for a surface defect. Vertical stripes on the rail head that are due to unavoidable specular reflections make the analysis more difficult.

Surface defects can also appear in dark zones of the rail head .

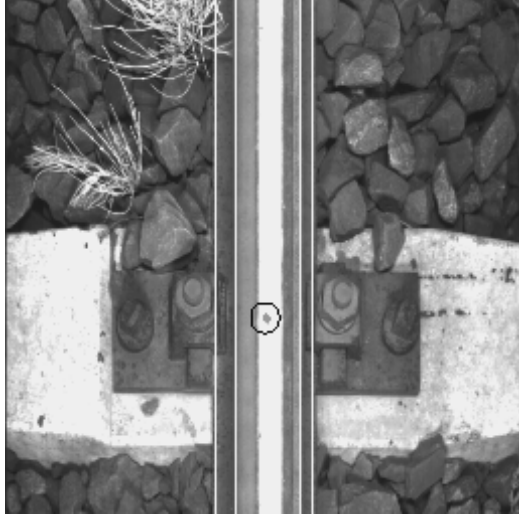


Fig. 2: Detected fault

Since the raw data, which have to be processed, are a set of images it is reasonable to adopt basic principles of human vision (cf. [5] and [6]) for the general analysis strategy. This has to be done in an efficient and simplified form in order to assure reliability and moderate computational complexity. Following this general guideline, feature extraction is performed at different resolution levels. Edge information is taken into account and local neighborhood-dependent features of objects are calculated. The relations between local and global image perception and the geometrical forms of objects are taken into account. Most of these tasks are performed by nonlinear operations. As far as possible, algorithms are designed for massively parallel computing.

## 2. RAIL HEAD LOCALIZATION

Due to vibrations of the train and thus fluctuating camera angles, positions of foot and head of the rail in the video images (cf. Fig. 2) vary which means that they have to be redetermined from frame to frame. A reliable localization of the rail head and its surface defects can only be realized by the analysis of features derived on the basis of a two-dimensional signal. Hence, the individual image lines generated by the camera are summarized to form frames of 256 x 256 pixels in size (cf. Fig. 2). On the basis of Gaussian and Laplacian image pyramids (cf. [1], [4], [8], and [11]) suitable features for head detection are derived in different resolution levels. The latter are computed by low pass filtering and sampling rate reduction. The features have been chosen in such a way that a two step procedure for the localization of the region of interest (ROI) is possible, which saves computation time. Surface characteristics as well

as edges of the rail have been taken into account. On the basis of the local edge density (cf. [1]) a raw rail localization is determined within a low resolution image level. This behavior is very robust with respect to illumination conditions and independent of the rails' gray value. In a second step, a high resolution level is used for the exact localization of the rail. Images are normalized by equalizing histograms (cf. [12]) so that textures and edges are improved. This operation leads to a normalization of the variance of the whole image and to a more homogeneous distribution of local signal variances. Large homogeneous regions of the image correspond to high histogram values and lead to a large magnification of the gray levels in this domain. However, equalizing the histogram also amplifies noise which makes an additional low-pass filtering necessary before edge detection can be performed.

Edge detection is performed by the application of the Marr-Hildreth operator (cf. [5]) which includes LoG-filtering and searching for zero crossings of the output signal. The LoG-filter represents a two-dimensional band pass and is of major importance in the processing of visual information by animals. For example, the receptive field of bipolar cells in the retina operates approximately like a LoG-filter (cf. [6]). Mathematically, a LoG-filter is equivalent to a Gaussian low-pass filter cascaded with the Laplace operator. In the first step, noise and very small structures are suppressed by the low-pass filter, and in the second, intensity variations (edges) are detected by means of the Laplace operator (cf. [5]). The latter is the isotropic derivative operator of the smallest order. Hence, its use for edge detection is very efficient (cf. [5]) compared to direction dependent gradient operators. Furthermore, the advantages of the LoG-filter, e.g. compared to the Sobel operator, have been confirmed by many computer simulations. The incorporated low-pass filter makes the Marr-Hildreth operator resistant with respect to anomalies in real data. In contrast to this, the use of the Sobel operator for edge detection implies the search for local maxima of the filter output signal which is relatively time consuming. In view of this fact, the Marr-Hildreth operator has been preferred which ensures that the signal is locally smoothed (low-pass filtering) and edges are marked at zero crossings of the filter output signal.

The localization of zero crossings leads to a binary edge image (cf. Fig. 3c) and represents a nonlinear operation. It extracts two-dimensional local geometric information like edge contours. Information concerning steepness of edges is hereby eliminated which is important for global image perception.

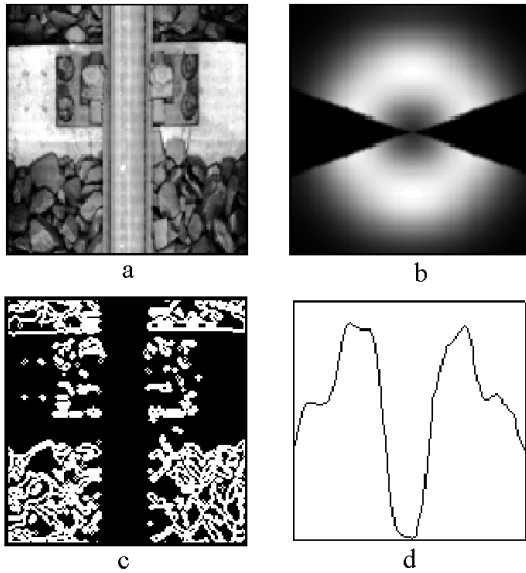


Fig.3: a) Original image,  
b) Frequency response of the filter,  
c) Binary edge contour,  
d) Smoothed edge projection.

Raw rail localization is based on a high resolution level. At this level, vertical disturbing stripes have to be suppressed by combining LoG-filtering with angular filtering. In Fig. 3b, the magnitude of the frequency response of this combined filter is depicted. For example, filtering of image a) in Fig. 3 in combination with the detection of zero crossings leads to the binary edge contour c). Subsequent low-pass filtering reveals the local edge density. Finally, the rail position can be localized by using the maxima of the vertically projected edge image. The low-pass filtering and projection operations can be interchanged. The low-pass filtered version of the vertically projected edge image is shown in Fig. 3 d) and its analysis permits the raw rail localization (definition of ROI) with respect to its horizontal position.

The exact positions of the edges of foot and head of the rail in the video images are determined in the domain of the already determined ROI. This is done on the basis of a high resolution level where four parallel lines (edges) are searched. For this purpose, vertical stripes caused by unavoidable specular reflections on the head have to be ignored which is done by taking into account only the first two lines on the left and right-hand side, respectively. More precisely, in the first step the histogram of the image is equalized and the result is filtered by a LoG-operator. The detection of the zero crossings is done in such a way that vertical edges are preferred. In general, line detection on the basis of an edge image can be implemented by means of local and global projections, respectively. Small angular

deviations of the rail from an exact vertical position can be neglected in this application which implies the simple use of column sums (vertical projections) for line detection. However, the edges of foot and head exhibit many breaks due to strong distortions. Furthermore, additional vertical edges appear in the images which are not caused by foot or head but for example by the fixing devices. In these cases, projections are not sufficient for a robust localization of foot and head of the rail. This problem is solved by using morphological line analysis (filtering) methods. The principles of these nonlinear processing schemes will be illustrated by discussing Fig. 4. Its first row shows the original edge image (Fig. 4a) and the results of morphological operations applied to it (Fig. 4b and c). The lower row shows the calculated vertical projection. First, the operation "closing" together with the structural element "short vertical line" (cf. Fig. 4b) is applied for closing short gaps in the edges of foot and rail head. Subsequently, the operation "opening" together with the structural element "long vertical line" is used for the elimination of short edges which cannot be caused by the rail edges (cf. Fig. 4c).

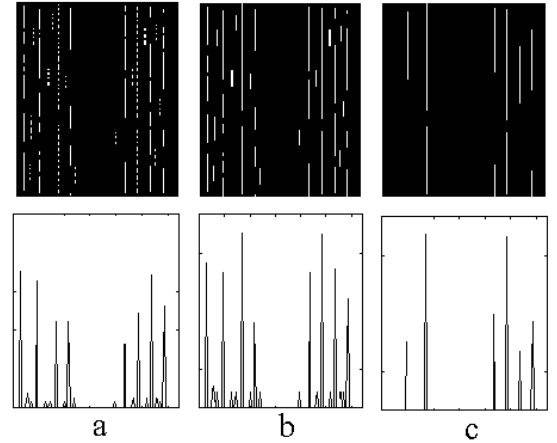


Fig. 4: Nonlinear processing of edge image.

Mathematically, the operations opening ( $\ominus$ ) and closing ( $\oplus$ ), respectively, can be formulated as [7]

$$O(b) = (b \ominus SE_L) \oplus SE_L,$$

$$C(b) = (b \oplus SE_L) \ominus SE_L,$$

where  $b$  is the binary image,  $SE_L$  the structural element "vertical line",  $\oplus$  stands for dilation, and  $\ominus$  for erosion.

### 3. TEMPORAL ON-LINE FILTERING

Individual errors of the algorithm described in the last section for the exact horizontal rail localization in the

image can be bridged by means of interframe filtering. The series of computed horizontal coordinates of the rail (one in each frame) can be considered as a discrete-time signal. The suppression of local errors would be possible by means of low-pass filtering. However, good filters with narrow transition bands have large group delays which leads to memory problems in an on-line system (many images have to be stored). For example, a causal linear phase FIR low-pass filter of the order  $N$  has a group delay of  $N/2$  samples, i.e., if we process image number  $i$ , then we obtain the filtered version of the rail position for image number  $i-N/2$ . Hence, the subsequent defect detection requires the storage of the last  $N/2$  images. Similar considerations apply to non-causal FIR low-pass filters. IIR filters with a narrow transition band can be designed with low order, however, they cannot have a linear phase. A better alternative is offered by the use of nonlinear median filters. For example, a median filter of the order five requires the storage of only three images and it is able to eliminate up to two errors in a sequence of five images. Experiments with real data showed that such a median filter of the order five is indeed sufficient for the application considered.

#### 4. RAIL INSPECTION

The rail head represents the region of interest for the localization of damage (cf. Fig. 5a). Latter can be identified due to the geometric forms and the difference from the surrounding with respect to gray level values.

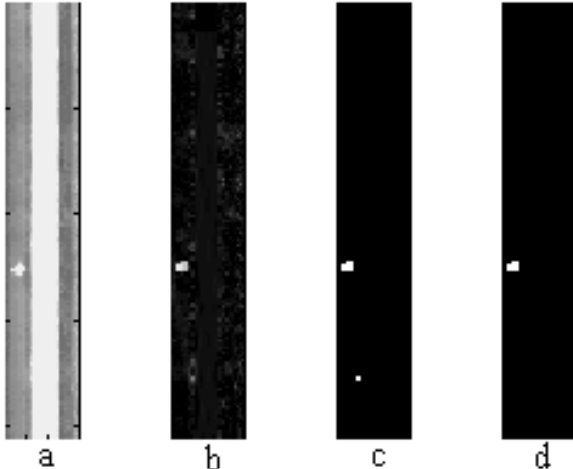


Fig. 5: Suppression of vertical stripes

The unavoidable specular reflections from the rail head lead to disturbing vertical stripes in the images (cf. Fig. 5a). They have to be eliminated by means of angular filtering. For this purpose, the already localized ROI (rail head) is divided into horizontal equi-

spaced stripes (blocks). The number of blocks depends on the expected maximum diameter of faults. Afterwards, angular filtering can be performed for all blocks in parallel. Here, filtering is carried out in the frequency domain on the basis of an FFT, which is approximately the same as subtracting its respective mean value from each column of a block. As a consequence, the filter output signal has positive and negative values which means that its magnitude has to be determined before a level detection operation can be performed. Afterwards, the background appears nearly homogeneous and its signal values cause a peak near to zero in the histogram. In contrast to this, the signal values stemming from damaged areas influence the histogram at higher values which are separated from the background peak. Hence, a suitable threshold for binarization can be easily defined. The geometrical properties of defects are enhanced in the binary image. Isolated white pixels can be interpreted as noise and are removed by means of a simple morphological operation. The remaining white domains are sorted with respect to its diameters since small patches on the surface are not considered as relevant faults (cf. Figs. 5c, 5d, and 6). Morphological sieve filtering [10] is used for the detection of objects which cannot be encircled by a circle of prescribed diameter. Mathematically, the filter itself can be described as follows [10]:

$$SF(b) = (b \oplus \lambda SE_C) \ominus \lambda SE_D,$$

where  $b$  is the binary image,  $\oplus$  stands for dilation,  $\ominus$  for erosion,  $\lambda$  represents a scaling factor,  $SE_C$  the structural element "circle", and  $SE_D$  the structural element "disk". The sieve filter performs a binary decision with respect to the diameter of objects, since it will be accepted or eliminated as a whole. The results of this nonlinear operation is illustrated in Fig. 6. Dependent on their size and the diameter  $D$  (in pixels) of the structural element, patches are accepted or eliminated.

#### 5. SPECIAL PURPOSE HARDWARE

The image analysis introduced above is based on two-dimensional filtering, FFT, morphological operations like dilation and erosion, equalization of histograms, and binarization. The parallel execution of operations is unavoidable in order to realize real time processing. However, special purpose chips and hardware modules are commercially available which execute the above tasks with specially designed architectures. In the present application, such modules can be implemented in a pipeline structure which makes a frame rate of 20 ms (256 lines per frame) possible. A delay of some frames between input and output of the analysis de-

vice is of no relevance. Thus, the algorithm can be separated into some sequentially ordered tasks, every single step may require up to 20 ms of execution time. Furthermore, some operations can be computed in parallel. For example, an image can be filtered with four different processors simultaneously.

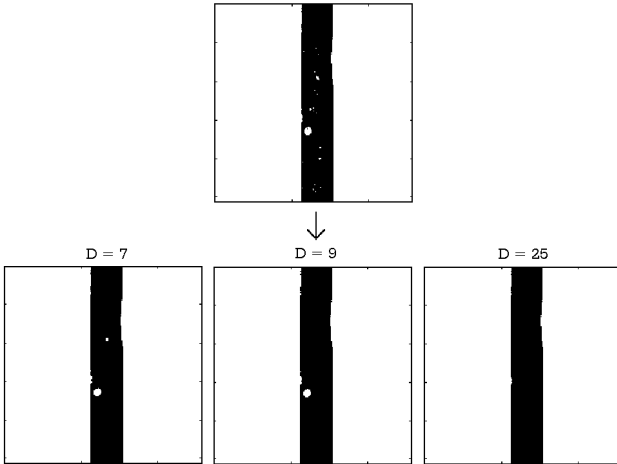


Fig. 6: Sieve filtering

## 6. CONCLUSIONS

The consistent use of principles of human vision and the exploitation of a priori knowledge leads to computationally fast and robust defect detection algorithms. Nonlinear signal processing operations are an essential part of the image analysis system introduced above. The efficiency and reliability of the methods have been verified by the analysis of large real data image sequences. The algorithms can be implemented for real time processing by means of available and commercially acceptable hardware modules.

## 7. REFERENCES

- [1] P.J. Burt, *The pyramid as a structure for efficient computation*. In A. Rosenfeld, editor, *Multiresolution Image Processing and Analysis*. Springer-Verlag, 1984.
- [2] P. Haberäcker, *Digitale Bildverarbeitung*. Hansen, München, Wien, 1991.
- [3] P. B. Hansen, *The nature of parallel programming*. In M.A. Arbib and J.A. Robinson, editors, *Natural and Artificial Parallel Computation*. The MIT Press, Cambridge, 1990.
- [4] J.S. Lim, *Two-Dimensional Signal and Image Processing*. Prentice-Hall, Englewood Cliffs, New Jersey 07632, 1990.
- [5] D. Marr, *Vision*. Freeman, San Francisco, 1982.
- [6] K. K. De Valois, R. L. De Valois, *Spatial Vision*. Oxford University Press, 1990.
- [7] X. Zhuang, R. M. Haralick, S. R. Sternberg, *Image analysis using mathematical morphology*. IEEE Trans., PAMI-9(4): 532-550, 1987.
- [8] B. Schneider, *Schnelle Merkmalsextraktion auf der Basis pyramidaler Bilddatenstrukturen für die Oberflächeninspektion*. Hanser, München, Wien, 1995.
- [9] STN ATLAS Elektronik GmbH, benotec Videokontrolltechnik GmbH. *RAIL CHECK Automated Inspection of Rail Networks*, Company Brochure, May 1996.
- [10] H.C. Tuczek, *Inspektion von Karosseriepreßteilen auf Risse und Einschnürungen mittels Methoden der Bildverarbeitung*. Springer-Verlag, Berlin, 1992.
- [11] D. Vollmerhaus, *Texturanalyse auf der Basis hierarchischer Bildpyramiden*. Hanser, München, Wien, 1992.
- [12] F.M. Wahl, *Digitale Bildsignalverarbeitung*. Springer-Verlag, 1984.